Published in final edited form as:
Biochemistry. 2009 August 25; 48(33): 8070–8076. doi:10.1021/bi901087z.

APOLIPOPROTEIN MODULATION OF STREPTOCOCCAL SERUM OPACITY FACTOR ACTIVITY AGAINST HUMAN PLASMA HIGH DENSITY LIPOPROTEINS

Corina Rosales[¶], **Baiba K. Gillard**[¶], **Harry S. Courtney**[§], **Francisco Blanco-Vaca**[†], and **Henry J. Pownall**[¶,*]

[¶]Section of Atherosclerosis and Vascular Medicine, Department of Medicine, Baylor College of Medicine, Houston, TX, 77030

[§]Veterans Affairs Medical Center and Department of Medicine, University of Tennessee Health Science Center, Memphis, TN 38104

[†]Department of Biochemistry, Hospital de la Santa Creu i Sant Pau and Universitat Autònoma de Barcelona, Barcelona 08025, Spain; CIBER de Diabetes y Enfermedades Metabólicas Asociadas4, Barcelona 08036, Spain

Abstract

Human plasma HDL are the target of streptococcal serum opacity factor (SOF), a virulence factor that clouds human plasma. Recombinant (r) SOF transfers cholesteryl esters (CE) from ~400,000 HDL particles to a CE-rich microemulsion (CERM), forms a cholesterol-poor HDL-like particle (neo HDL), and releases lipid-free (LF) apo A-I. Whereas the rSOF reaction requires labile apo A-I, the modulation effects of other apos is not known. We compared the products and rates of the rSOF reaction against human HDL and HDL from mice over expressing apos A-I and A-II. Kinetic studies showed that the reactivity of various HDL species is apo-specific. LpA-I reacts faster than LpA-I/A-II. Adding apos A-I and A-II inhibited the SOF reaction, an effect that was more profound for apo A-II. The rate of SOF-mediated CERM formation was slower against HDL from mice expressing human apos A-I and A-II than against WT mice HDL, and slowest against HDL from apo A-II over expressing mice. The lower reactivity of SOF against HDL containing human apos is due to the higher hydropathy of human apo A-I, particularly its C-terminus relative to mouse apo A-I, and the higher lipophilicity of human apo A-II. The SOF-catalyzed reaction is the first to target HDL rather than its transporters and receptors in a way that enhances reverse cholesterol transport (RCT). Thus, effects of apos on the SOF reaction are highly relevant. Our studies show that the "humanized" apo A-I-expressing mouse is a good animal model for studies of rSOF effects on RCT in vivo.

Keywords

High density lipoprotein; reverse cholesterol transport; serum opacity factor; atherosclerosis

Plasma HDL are vehicles for reverse cholesterol transport (RCT), the transfer of cholesterol from peripheral tissue to the liver for recycling or disposal (1,2). HDL comprise a core of mostly CE surrounded by a surface monolayer of free cholesterol (FC), phospholipids (PL), and specialized proteins- apolipoproteins (apos) A-I and A-II (3). Immunochemical methods

Address correspondence to: Henry J. Pownall, PhD, One Baylor Plaza, MS A601, Houston Texas 77030, Phone: 713-798-4160, Fax: 713-798-9005.

have been used to separate HDL into LpA-I, (apo A-I but not apo A-II), and LpA-I/A-II, (apos A-I and A-II), both of which have α mobility, contain apos C, D, and E as well as LCAT, and exhibit size heterogeneity; the LpA-I/A-II have an apo A-I/apo A-II molar ratio of ~2:1. LpA-I and LpA-I/A-II are biologically distinct. The plasma residence time of apoA-I on LpA-I is shorter than that on LpA-I/A-II suggesting divergent metabolic pathways (4). LpA-I is a better acceptor of cell derived cholesterol than LpA-I/A-II and a better LCAT substrate (5). LpA-I but not LpA-I/A-II is reduced in normolipemic patients with coronary artery disease when compared to asymptomatic subjects (6). Compared to young subjects, LpA-I is elevated and LpA-I/A-II is reduced in octagenerians (7). The inverse correlation of LpA-I with myocardial infarction is slightly stronger than that of LpA-I/A-II (8).

SOF, a protein produced by *Streptococcus pyogenes*, causes serum and plasma to cloud, i.e., opacify, a process that involves the binding of SOF to HDL and the liberation of apos (9). SOF is large, multifunctional protein that is covalently bound to the streptococcal surface via an LPXXG sortase recognition site and is also released in a soluble form. In addition to its ability to opacify serum, SOF has a direct role in mediating adhesion to and invasion of host cells (10,11). SOF binds to extracellular matrix proteins such as fibronectin (12, 13), fibrinogen (14), and fibulin-1 (15) and these binding activities are thought to play a major part in the adhesion of *S. pyogenes* to host surfaces. However, the opacification and adhesion-mediating activities of SOF have been shown to be functionally discrete (16).

SOF specifically targets HDL in serum to induce opacification and according to chemical kinetics; it is a heterodivalent fusogen that catalyzes the disproportionation of HDL into a large CERM and neo HDL, a small, discoidal HDL-like particle with mobility, with the concomitant release of LF apo A-I but not apo A-II (17). The rate and magnitude of opacification increases with HDL size, presumably because large HDL contain more neutral lipid, the essential opacification component that is transferred to the CERM (17). Given that HDL instability, particularly apo A-I lability, appears to be inextricably linked to the opacification mechanism, we hypothesized that apo A-II would stabilize HDL to opacification. This hypothesis was tested by product and kinetic analysis of the reaction of rSOF against HDL that varied in their apo A-II content. These included: LpA-I and LpA-I/A-II, isolated from human plasma by a new simple method; apo A-II-rich human HDL formed by the displacement of apo A-I by apo A-II; and apo A-II-rich and -poor HDL from mice over- expressing human apos A-I and A-II. Our results show that apo A-II stabilizes HDL except at very high, non physiological HDL-apo A-II content. This work, defining apo A-II stabilization of HDL to opacification by SOF, provides a basis for evaluating the anti-atherogenic potential of the opacification reaction that is catalyzed by SOF and perhaps other rationally designed therapeutic agents that catalyze opacification.

Experimental Procedures

Apo A-I, apo A-II and rSOF

Apos A-I and A-II were isolated from human plasma HDL as described previously (18). A polyhistidine-tagged, truncated form of sof2, rSOF, encoding amino acids 38–843 was cloned and expressed in Escherichia coli and purified by metal affinity chromatography (9,13).

HDL purification and subfractionation

HDL was isolated from human plasma from The Methodist Hospital Blood Donor Center by sequential flotation at d = 1.063 and 1.21 g/mL. The HDL were further purified by size exclusion chromatography (SEC). For some tests HDL were subfractionated according to size by SEC using two Superose HR 6 columns (GE Healthcare, Piscataway, NJ) in tandem

(17, 19). Fractions from multiple injections (0.5 mL) were pooled as needed for kinetic analysis. All HDL species eluted as a single SEC peak.

LpA-I and LpA-I/A-II purification

LpA-I and LpA-I/A-II were isolated from human HDL by covalent chromatography on Thiopropyl Sepharose (GE Healthcare). This protocol takes advantage of the Cys-6 in human apo A-II and the absence of Cys in human apo A-I, so that LpA-I flows through the column while reduced LpA-I/A-II binds. LpA-I/A-II is recovered by treating the column with dithiothreitol (DTT). TPS (2 g) was stirred into deionized water (6 mL) for 15 min, poured into a 1 cm × 10 cm column equipped with a stopcock and washed with deionized water (400 mL). The washed beads were resuspended in 16 mL TBS and divided into two equal aliquots. One aliquot was stirred with HDL (100 mg in 15 mL); the other was returned to the column. After 20 min, the HDL-TPS mixture was layered on top of the TPS column and allowed to settle. Ten 2-mL fractions containing LpA-I were eluted with TBS and collected. The column was washed with 50 mL TBS and the effluent discarded. The absorption spectrum of a 1:10 dilution of the TBS after-wash should show no protein indicating that non-bound LpA-I has been eluted from the column. 40 mL DTT (20 mM) was added to the column and 10 3-mL fractions were collected, some of which contained reduced LpA-I/A-II. The absorption spectrum of each fraction was used to verify the elution of LpA-I and LpA-I/A-II based on the emission maxima of 280 nm for apo A-I and 276 nm for apo A-II (20). SDS-PAGE under reducing conditions revealed a single apo A-I protein band for LpA-I and two bands for LpA-I/A-II, apo A-I and monomeric apo A-II. The fractions with the highest protein concentration were combined and dialyzed for >2 days in TBS, during which apo A-II redimerizes as confirmed by SDS-PAGE. LpAI and LpAI/AII were concentrated by flotation at 1.21 g/mL. The weight ratio of isolated LpAI to LpAI/AII was ~2.

Transgenic mouse HDL and human apo A-II enriched HDL

HDL were isolated from the plasma of mice overexpressing human apo A-I, and high (Hi) and low (Lo) levels of human apo A-II which have been described and designated 11.1 and 25.3, respectively (21). The total lipoproteins of 2–4 mL of plasma were floated for 48 h at d = 1.21 g/mL after which the narrow cloudy layer at the top of the centrifuge tube, ~0.7 mL, was transferred to a second centrifuge tube overlaid with d = 1.063 g/mL, and centrifuged for an additional 18 h. The lipoproteins at the top of the tube were removed and discarded; the bottom 0.5 – 1.0 mL was removed with a 9" Pasteur pipette which passed through the supernatant to the bottom of the tube. Both spins were at 50,000 rpm in a Beckman SW 55 Ti rotor. Human HDL was enriched with apo A-II by displacement of apo A-I as previously described (22). Additional details on various HDL subfraction compositions are in the Figure legends.

Analysis of rSOF Activity by SEC

Various amounts of HDL and rSOF were combined at 37° C. At the end of each incubation, an aliquot (0.2 mL) was analyzed by SEC using an Amersham-Pharmacia ÄKTA chromatography system equipped with two Superose HR6 columns in tandem and eluted with TBS at a flow rate of 0.45 mL/min.

Western blotting

SEC fractions were analyzed for apos by Western blotting. Proteins were resolved on 18% Tris-glycine Precast Gels (Invitrogen) by SDS-PAGE and transferred to nitrocellulose for immunoblotting. The Western blotting method was performed according to Amersham ECL-plus manual specifications (Amersham GE Healthcare). Immunoblots were conducted

with HRP-conjugated goat anti-human apo A-I and apo A-II from Academy Biomedical (Houston, TX). These antibodies are highly specific for human apos and do not cross react with mouse apos.

Kinetic Turbidimetry

The rates of rSOF-mediated opacification of HDL were measured as a function of time by kinetic turbidimetry which monitors light scattering produced by the appearance of the very large (>100 nm) CERM particle (23). After thermal pre-equilibration of HDL (0.5 mg/mL) at 37° C, rSOF (1 μg/mL) was added and the increase in right angle scattering light intensity was measured at 325 nm as a function of time on a Jobin Yvon Fluorolog. The intensity vs. time data were fitted to the growing exponential function, $It = I0 + a(1 - e^{-kt})$, where I0 is the initial scattering intensity, It is the intensity as a function of time (t), a is a pre exponential instrumental factor and k is the rate constant.

Results

Characterization of HDL Species

The various human and mouse HDL species were analyzed by SDS-PAGE Western blotting (Figure 1). As expected, LpA-I contains apo A-I but is practically devoid of apo A-II whereas LpA-I/A-II contains both apos A-I and A-II (Figure 1A). SDS-PAGE of the mouse HDL species confirmed their respective phenotypes (Figure 1B). HDL from WT and human apo A-I (+) mice contained a prominent band for apo A-I. According to SDS-PAGE, HDL from the apo A-II (Lo) mouse contains apo A-I and a small amount of human apo A-II. A similar analysis of HDL from the apo A-II (Hi) mouse showed a prominent band for both apo A-I and apo A-II. Immunoblot analysis of WT mouse HDL shows the total absence of antibody binding, confirming the specificity of the antibodies for human apos. In contrast, the HDL from transgenic mice expressing human apo A-I is positive for apo A-I but not human apo A-II; similarly, HDL from mice overexpressing human apo A-II is positive for human apo A-II but not apo A-I.

To test the effects of human apo A-II on the reactivity of HDL to rSOF, we studied the reaction of rSOF against HDL by SEC and kinetic turbidimetry. The HDL contained varying amounts of apo A-II: (1) human HDL with and without apo A-II; (2) HDL that contained different amounts of apos via the addition of exogenous apos; and (3) HDL from mice expressing human apo A-I or apo A-II. These HDL species were compared by SEC, which revealed the compositions of the HDL pre and post incubation with rSOF, and by kinetic turbidimetry, which reflected HDL stability to rSOF according the rate of CERM formation.

LpA-I and LpA-I/A-II

Both SEC and turbidimetric kinetics revealed differences between LpA-I and LpA-I/A-II reactivity. Previous studies (17), indicated that rSOF activity against total HDL released nearly half of the HDL protein as LF apo A-I. Our control data (Figure 2A) confirms this previous finding. In contrast, LpA-I released less and LpA-I/A-II released more apo A-I than control HDL. The percentage of LF A-I formed from HDL, LpAI, and LpAI/AII was 47%, 42%, and 51%, respectively ($p \geq 0.005$). Thus, according to the amount of apo A-I released, LpA-I/A-II contains more rSOF-releasable apo, i.e., labile apo A-I than does LpA-I. As expected, the amount of LF apo A-I formed from total HDL in response to rSOF is between that of its components, LpA-I and LpA-I/A-II. These data were corroborated by kinetic turbidimetry, which reflects the rate of CERM formation. The rate of CERM formation from LpA-I was twice as fast as that from LpA-I/A-II (Figure 3).

Effect of excess LF apos

In vitro addition of apo A-II to HDL displaces apo A-I giving rise to an apo A-II-rich HDL particle (22). Thus we compared the activity of rSOF on HDL to which exogenous apos had been added to alter HDL apo composition. Addition of apos A-I and A-II to HDL gave distinct products. Addition of apo A-I did not displace any apo A-II at either concentration but only appeared to slightly enrich HDL with apo A-I (Figures 4B, 4C). However, subsequent treatment with rSOF to the A-I enriched HDL did release a small amount of apo A-II at the higher apo A-I concentration (Figure 4C). Addition of apo A-II gave the expected dose-dependent displacement of HDL-apo A-I (22), with partial displacement of apo A-I at 0.05 mg/mL apo A-II (Figure 4D) and total displacement at 0.23 mg/mL (Figure 4E).

According to the magnitude of the peak in the void volume of the SEC, enrichment of HDL with apos A-I and A-II produced a nominal but similar reduction in CERM formation. In contrast, the effects of rSOF on apos A-I- and A-II-enriched HDL were distinct. Relative to HDL, addition of rSOF to apo A-I enriched HDL produced LF apo A-II, an effect that increased from nil at low apo A-I/HDL ratios to a prominent apo A-II-positive band at a higher ratio (~0.5) (Figure 4 B and C, lower immunoblots). The effect of similar HDL enrichment with apo A-II, was much more profound. Even at a low apo A-II to HDL ratio (~1:10), rSOF catalyzed the release of LF apo A-I (Figure 4 D) and at an apo A-II/HDL ratio of 0.5, Virtually all of the apo A-I was released as LF apo by rSOF (Figure 4 E). These data show that apo addition to HDL reduces CERM formation but enhances rSOF-mediated LF apo release.

The effects of adding excess LF apo to HDL on the rate of CERM formation were assessed by kinetic turbidimetry with the addition of up to 2.7 mg apo/mg HDL both the rate and magnitude of opacification were reduced in a dose-dependent way (Figure 5A, 5B). The effect of apo A-I reached a maximum by 0.23 mg/mL, while addition of apo A-II continued to decrease both the rate and maximum opacification at 0.67 mg/mL. The reduction in opacification rate with the addition of apo A-II (-7.2×10^{-3} $sec^{-1}mg^{-1}$) was twice that for apo A-I (-3.8×10^{-3} $sec^{-1}mg^{-1}$) (Figure 5C). Based on the fit to the kinetic data, addition of apo A-II reduced the magnitude of the opacification over 5 times more than did addition of apo A-I-(~25% vs ~ 80%) (Figure 5D).

Activity of rSOF against HDL from Mice with Genetically-altered Apo Expression

The SEC of HDL isolated from WT, apo A-I (+), apo A-II (Lo), and apo A-II (Hi) mice showed that HDL from mice expressing human apos were larger than that of WT. In response to rSOF treatment, the HDL from all four mouse types exhibited similarly robust opacification. Unlike human HDL, the LF apo A-I peak from WT mouse HDL appears as a shoulder on the neo HDL peak that has much lower intensity than that of LF apo A-I formed by the activity of rSOF against human HDL (Figure 6A). The activity of rSOF against HDL from mice expressing human apo A-I, ApoA-I (+), released more LF apo A-I than HDL from WT mice. In contrast, the release of LF apos by mice expressing small amounts of human apo A-II is similar to that of WT. Of the mouse HDL tested, opacification of HDL from mice over expressing high levels of apo A-II was distinguished by the highest levels of LF apo release. Kinetic Turbidimetry of rSOF against HDL from Mice with Genetically-altered Apo Expression: Kinetic turbidimetry of rSOF activity against the HDL of mice expressing human apos A-I and A-II revealed differences that included differences in both the rates and magnitude of opacification (Figure 7A). The initial rate of opacification was highest for HDL from WT mice and decreased in the order WT (~8.8) > apo A-I (+) (~7) > apo A-II (Lo) (~5) > apo A-II (Hi) (~1) (Figure 7B), indicating that both human A-I and A-II stabilize mouse HDL to rSOF, and that this stabilizing effect is more profound with high amounts of human apo A-II (Figure 7B). The magnitude of opacification was lower for HDL

from WT mice and A-II (Hi) than for apo A-I (+) HDL and apo A-II (Lo) HDL (Figure 7C). Since the SEC data of Figure 6 show that all these opacification reactions go to completion, the lower opacification max may be due to formation of smaller CERM particles, resulting in lower scattering intensity.

Discussion

Analysis of the Products of the SOF Reaction

According to SEC, the amount of CERM and LF apo formed are a function of the HDL compositions. Whereas there was little difference in the profiles for HDL, LpA-I, and LpA-I/A-II before incubation with rSOF, treatment with rSOF gave rise to differences, the most prominent being that LpA-I/A-II released more LF apo A-I than did LpA-I. This occurred despite the lower apo A-I content of LpA-I/A-II. We conclude that the occurrence of human apo A-II on native human HDL is associated with more apo A-I within the rSOF-releasable apo pool.

The effects of apos were further tested by studies of HDL pre incubated with apos A-I and A-II, and analyzed by SEC before and after incubation with rSOF. Pre incubation of HDL with apo A-I or apo A-II had no effect on the amount of CERM produced. The same was not true of the amount of LF apo released in response to rSOF (Figure 4). Whereas separate treatment of HDL with apo A-I or rSOF alone did not release any apo A-II to the LF fraction, the successive treatment of HDL with higher concentrations of apo A-I and with rSOF transferred some of the apo A-II into the rSOF-releasable pool (Figure 4A-C). The effects of apo A-II were more profound. Although HDL in the presence of a low concentration of apo A-II retained all of its apo A-I (upper immunoblot, Figure 4D), incubation with rSOF released nearly all apoA-I to the LF pool (Figure 4D, lower immunoblot; compare fractions 32, 33 to 34, 35). This contrasts to control HDL, in which ~50% of the apo A-I remains in the neo HDL fractions (Figure 4A, lower immunoblot). Thus, addition of apo A-II to HDL not only displaces apo A-I but also transfers additional apo A-I to the rSOF-releasable pool.

At the higher concentration of apo A-II, nearly all apo A-I was displaced from HDL (upper immunoblot, Figure 5E). This A-II-rich HDL was still rSOF-reactive, forming CERM, which appears in the void volume, a neo HDL with a trace of apo A-I, and leaving an A-II rich-neo HDL that elutes between 31 and 33 mL. We conclude that addition of excess apo A-I to HDL effects rSOF release of apo A-II into the LF pool. Thus, addition of apos A-I and A-II to HDL, transfers additional apo A-II and A-I respectively to the rSOF-releasable apo pool.

SEC of the mouse HDL shows that WT mice have smaller HDL compared to that of mice expressing human apos A-I and A-II. SEC also shows that less CERM is formed from the HDL of WT mice than from the other mice. This is a size effect that is a function of the CE content, and is consistent with our previous observations on various HDL subfractions of different size and CE content (17). Large HDL contain more CE than small HDL and given that CE is the major component of the CERM, it is expected that more CERM is formed from the larger more CE-rich transgenic mouse HDL.

There were other notable differences. First, the amount of LF apo A-I released by the HDL from WT mice was much lower than that from human HDL (compare Figure 2A and 6A). However, comparison of the SEC of the post rSOF of HDL from WT mice with that of the apo A-I (+) mice shows an increase in the amount of LF apo A-I produced by "humanizing" mouse HDL. There was little difference between the effects of rSOF on HDL from WT and the apo A-II (Lo) mice. This is likely because the amount of human apo A-II in the HDL of

these mice is very low (Figure 1). In contrast, there was a robust rSOF-mediated release of LF apo from the HDL of the apo A-II (Hi) mice. These data complement the studies with added apo A-I and A-II, and the comparison of LpA-I with LpA-I/A-II by showing that the addition of apo A-II increases the rSOF-releasable apo pool.

Apo A-II Inhibition of SOF Reaction Kinetics

Collectively, our findings show that in the segue from physiological-LpA-I vs. LpA-I/A-II- to the more mechanistic-apo add-back to HDL and HDL from mice over expressing apos (Figures 3, 5, and 7, respectively), the occurrence of apo A-II in HDL is associated with a reduced rate of opacification, an effect that persists even when comparing the add-back of apo A-I to that of apo A-II (Figure 5). As with SOF, apoA-II inhibits the remodeling of HDL by other physiologically important factors found in plasma, including lecithin:cholesterol acyltransferase and lipid transfer proteins (24–27), an effect that others have assigned to a direct stabilizing action of apoA-II on HDL. Although this conclusion is supported by studies (28) showing that apo A-II has a higher surface pressure before collapse in artificial monolayers than apo A-I, i. e., more stable, the effect is modest (~10%) and likely too small to explain the profound effects of apo A-II on SOF reaction kinetics. Moreover, recent denaturation studies (29) showed that LpA-I/A-II stability is comparable to if not slightly less than that of LpA-I, a finding that is also consistent with studies of rHDL (30–33). Another alternative is that addition of apo A-II alters the surface properties of HDL lipids. However, following the addition of human apo A-II to human HDL, we observed no change in the general polarization of Laurdan, a sensitive probe of lipid surface polarity (data not shown).

Our alternative explanation is that apo A-II displaces the one quality of HDL that is essential for the SOF reaction and that is labile apo A-I, which has a SOF-competent conformation that is distinct from that of apo A-I that remains bound after displacement with apo A-II (23). This conclusion is consistent with differential scanning calorimetry, circular dichroism, light scattering and electron microscopy data that shows that apoA-I occurs in two distinct populations on HDL that manifest themselves in the two successive thermal transitions: a labile population that dissociates concomitantly with HDL fusion, and a tightly bound population that dissociates upon HDL disintegration, rupture and release of a polar core (29).

Differential Effects of Mouse and Human Apo A-I

The kinetics of the SOF reaction against HDL containing human apo A-I was much slower than that of HDL from WT mice. Clues identifying the underlying differences between HDL from WT and human apo A-I over expressing mice were provided by the thermodynamic studies of Saito et al. (26), who found relevant differences in the compositions and properties of their C-termini. Both human and mouse apo A-I adopt a two-domain tertiary structure, analogous to that of apo E (26). In this model, mouse apo A-I residues 1–186 form an antiparallel helix bundle while residues 187–240 fold into a separate, disordered domain. The N- and C-terminal domains of mouse and human apo A-I are 70% and 46% identical, respectively (34), and the C-terminal 22-residue segments have only 30% sequence identity. These differences convey different properties to human and mouse apo A-I. According to the calculated mean residue hydropathy (34), mouse apo A-I is lower, i.e., more polar and less lipophilic than human apo A-I. This difference is profound for the 54 C-terminal residues of human vs. and mouse apo A-I for which the consensus scale gives values of −0.17 and −0.25 kcal/mol for the C-terminal domains of human and mouse apo A-I, respectively. Since more negative values indicate higher polarity, the mouse peptide is more polar, i.e., less lipophilic.

According to denaturation studies, LF human apo A-I is more stable than LF mouse apo A-I (35) and the difference resides in the greater stability of the N-terminal helix bundle of human apoA-I, which has greater α-helical content. In the context of the essential and rate-limiting (23) role of apo A-I release, it is valuable to compare our SOF kinetic data with studies of lipid-binding kinetics by human and mouse apo A-I because this reaction involves the reverse of the SOF reaction, i.e., phospholipid-apo A-I association (35) vs. its dissociation during opacification. Again these data show that differences in lipid-binding reside in the C-terminus. The rate of lipid binding increases in the order of human apoA-I (1–189) < whole human apo A-I < human apoA-I (190–243). Thus, the C-terminal domain of human apo A-I is the most lipophilic, i.e., high affinity lipid binding. In contrast, the C-terminal domain of mouse apoA-I (residues 187–240) is disordered, much more polar, and binds lipids more slowly, i.e., is less lipophilic. Thus, the reverse process in the opacification reaction, apo A-I desorption, would be expected to be faster, as observed, for WT mouse HDL vs. human apo A-I (+) (Figures 7 and 8).

The broad goals of our studies with rSOF are to determine if the SOF reaction could be the basis of a new therapy to promote RCT. Opacification of HDL by rSOF produces CERM, neo HDL and LF apo A-I, all of which could enhance various RCT steps. With its high CE and apo E content (17), the CERM might be a vehicle for the hepatic clearance of large quantities of cholesterol as CE; neo HDL, which is phospholipid-rich and cholesterol-poor, should be a better acceptor of cellular cholesterol efflux. Lastly, LF apo A-I is a known ligand for efflux via ABCA1. The successive steps in testing whether the rSOF reaction has therapeutic potential requires studies in valid mouse models of human HDL metabolism. Based on the work presented here, the apo A-I (+) mouse which has a "humanized" post SOF SEC profile is our best model to date. Future studies of the roles of other apos and of atheroprotection in these and atherosusceptible mice could guide the rSOF reaction to human therapy.

Acknowledgments

Supported in part by grants-in-aid from the National Institutes of Health (HL 30914 and HL056865, HJP) and the Department of Veterans Affairs (HSC). CIBER de Diabetes y Enfermedades Metabólicas Asociadas is a ISCIII project.

Abbreviations

apo	apolipoprotein
LF	lipid-free
rSOF	recombinant serum opacity factor
HDL	high density lipoproteins
PL	phospholipid
CE	cholesteryl ester
PC	phosphatidylcholine
CERM	cholesteryl ester-rich microemulsion
SEC	size exclusion chromatography
RCT	reverse cholesterol transport
TBS	tris-buffered saline
LpA-I	HDL with apo A-I, without apo A-II

LpA-I/A-II HDL with apos A-I and A-II

REFERENCES

1. Cuchel M, Rader DJ. Macrophage reverse cholesterol transport: key to the regression of atherosclerosis. Circulation. 2006; 113:2548–2555. [PubMed: 16735689]
2. Curtiss LK, Valenta DT, Hime NJ, Rye KA. What is so special about apolipoprotein AI in reverse cholesterol transport? Arterioscler Thromb Vasc Biol. 2006; 26:12–19. [PubMed: 16269660]
3. Havel RJ, Goldstein JL, Brown MS. Lipoproteins in Lipid Transport. 1980:398–494.
4. Rader DJ, Castro G, Zech LA, Fruchart JC, Brewer HB Jr. In vivo metabolism of apolipoprotein A-I on high density lipoprotein particles LpA-I and LpA-I,A-II. J Lipid Res. 1991; 32:1849–1859. [PubMed: 1770304]
5. Huang Y, von Eckardstein A, Wu S, Assmann G. Cholesterol efflux, cholesterol esterification, and cholesteryl ester transfer by LpA-I and LpA-I/A-II in native plasma. Arterioscler Thromb Vasc Biol. 1995; 15:1412–1418. [PubMed: 7670956]
6. Puchois P, Kandoussi A, Fievet P, Fourrier JL, Bertrand M, Koren E, Fruchart JC. Apolipoprotein A-I containing lipoproteins in coronary artery disease. Atherosclerosis. 1987; 68:35–40. [PubMed: 3120739]
7. Amouyel P, Isorez D, Bard JM, Goldman M, Lebel P, Zylberberg G, Fruchart JC. Parental history of early myocardial infarction is associated with decreased levels of lipoparticle AI in adolescents. Arterioscler Thromb. 1993; 13:1640–1644. [PubMed: 8218104]
8. Stampfer MJ, Sacks FM, Salvini S, Willett WC, Hennekens CH. A prospective study of cholesterol, apolipoproteins, and the risk of myocardial infarction. N Engl J Med. 1991; 325:373–381. [PubMed: 2062328]
9. Courtney HS, Zhang YM, Frank MW, Rock CO. Serum opacity factor, a streptococcal virulence factor that binds to apolipoproteins A-I and A-II and disrupts high density lipoprotein structure. J Biol Chem. 2006; 281:5515–5521. [PubMed: 16407233]
10. Oehmcke S, Podbielski A, Kreikemeyer B. Function of the fibronectin-binding serum opacity factor of Streptococcus pyogenes in adherence to epithelial cells. Infect. Immun. 2004; 72:4302–4308. [PubMed: 15213180]
11. Timmer AM, Kristian SA, Datta V, Jeng A, Gillen CM, Walker MJ, Beall B, Nizet V. Serum opacity factor promotes group A streptococcal cell invasion and virulence. Mol Micro. 2006; 62:15–25.
12. Rakonjac JV, Robbins JC, Fischetti VA. DNA sequence of the serum opacity factor of group A streptococci: Identification of a fibronectin-binding repeat domain. Infect. Immun. 1995; 63:622–631. [PubMed: 7822031]
13. Courtney HS, Hasty DL, Li Y, Chiang HC, Thacker JL, Dale JB. Serum opacity factor is a major fibronectin-binding protein and a virulence determinant of M type 2 Streptococcus pyogenes. Mol Microbiol. 1999; 32:89–98. [PubMed: 10216862]
14. Courtney HS, Dale JB, Hasty DL. Mapping the fibrinogen-binding domain of serum opacity factor of group A streptococci. Curr. Microbiol. 2002; 44:236–240. [PubMed: 11910491]
15. Courtney HS, Li Y, Twal WO, Argraves WS. Serum opacity factor is a streptococcal receptor for the extracellular matrix protein fibulin-1. J. Biol. Chem. 2009; 284:12966–12971. [PubMed: 19276078]
16. Gillen C, Courtney HS, Schulze K, Rohde M, Wilson MR, Timmer AM, Guzman CA, Nizet V, Chhatwal GS, Walker MJ. Opacity factor activity and epithelial cell binding by the serum opacity factor protein of Streptococcus pyogenes are functionally discrete. J. Biol. Chem. 2008; 283:6359–6366. [PubMed: 18180300]
17. Gillard BK, Courtney HS, Massey JB, Pownall HJ. Serum opacity factor unmasks human plasma high-density lipoprotein instability via selective delipidation and apolipoprotein A-I desorption. Biochemistry. 2008; 46:12968–12978. [PubMed: 17941651]

18. Massey JB, Gotto AM Jr, Pownall HJ. Dynamics of lipid-protein interactions. Interaction of apolipoprotein A-II from human plasma high density lipoproteins with dimyristoylphosphatidylcholine. J Biol Chem. 1980; 255:10167–10173. [PubMed: 6776110]
19. Pownall HJ. Remodeling of human plasma lipoproteins by detergent perturbation. Biochemistry. 2005; 44:9714–9722. [PubMed: 16008356]
20. Pownall HJ, Massey JB. Methods in Enzymology. 1986; 128:515–518.
21. Marzal-Casacuberta A, Blanco-Vaca F, Ishida BY, Julve-Gil J, Shen J, Calvet-Marquez S, Gonzalez-Sastre F, Chan L. Functional lecithin:cholesterol acyltransferase deficiency and high density lipoprotein deficiency in transgenic mice overexpressing human apolipoprotein A-II. J Biol Chem. 1996; 271:6720–6728. [PubMed: 8636092]
22. Edelstein C, Halari M, Scanu AM. On the mechanism of the displacement of apolipoprotein A-I by apolipoprotein A-II from the high density lipoprotein surface. Effect of concentration and molecular forms of apolipoprotein A-II. J Biol Chem. 1982; 257:7189–7195. [PubMed: 6806266]
23. Han M, Gillard BK, Courtney HS, Ward K, Rosales C, Khant H, Ludtke SJ, Pownall HJ. Disruption of human plasma high-density lipoproteins by streptococcal serum opacity factor requires labile apolipoprotein A-I. Biochemistry. 2009; 48:1481–1487. [PubMed: 19191587]
24. Blanco-Vaca F, Escola-Gil JC, Martin-Campos JM, Julve J. Role of apoA-II in lipid metabolism and atherosclerosis: advances in the study of an enigmatic protein. J Lipid Res. 2001; 42:1727–1739. [PubMed: 11714842]
25. Calabresi L, Lucchini A, Vecchio G, Sirtori CR, Franceschini G. Human apolipoprotein A-II inhibits the formation of pre-beta high density lipoproteins. Biochim Biophys Acta. 1996; 1304:32–42. [PubMed: 8944748]
26. Saito H, Dhanasekaran P, Nguyen D, Holvoet P, Lund-Katz S, Phillips MC. Domain structure and lipid interaction in human apolipoproteins A-I and E, a general model. J Biol Chem. 2003; 278:23227–23232. [PubMed: 12709430]
27. Rye KA, Wee K, Curtiss LK, Bonnet DJ, Barter PJ. Apolipoprotein A-II inhibits high density lipoprotein remodeling and lipid-poor apolipoprotein A-I formation. J Biol Chem. 2003; 278:22530–22536. [PubMed: 12690114]
28. Krebs KE, Ibdah JA, Phillips MC. A comparison of the surface activities of human apolipoproteins A-I and A-II at the air/water interface. Biochim Biophys Acta. 1988; 959:229–237. [PubMed: 3128334]
29. Gao X, Yuan S, Jayaraman S, Gursky O. Differential stability of high-density lipoprotein subclasses: effects of particle size and protein composition. J Mol Biol. 2009; 387:628–638. [PubMed: 19236880]
30. Durbin DM, Jonas A. The effect of apolipoprotein A-II on the structure and function of apolipoprotein A-I in a homogeneous reconstituted high density lipoprotein particle. J Biol Chem. 1997; 272:31333–31339. [PubMed: 9395462]
31. Jayaraman S, Gantz DL, Gursky O. Kinetic stabilization and fusion of apolipoprotein A-2:DMPC disks: comparison with apoA-1 and apoC-1. Biophys J. 2005; 88:2907–2918. [PubMed: 15681655]
32. Swaney JB, Palmieri E. Hybrid association between human apolipoproteins A-I and A-II in aqueous solution and in phospholipid recombinants. Biochim Biophys Acta. 1984; 792:164–171. [PubMed: 6421327]
33. Reijngoud DJPMC. Mechanism of dissociation of human apolipoproteins A-I, A-II, and C from complexes with dimyristoylphosphatidylcholine as studied by thermal denaturation. Biochemistry. 1984; 23:726–734. [PubMed: 20815113]
34. Brouillette CG, Anantharamaiah GM, Engler JA, Borhani DW. Structural models of human apolipoprotein A-I: a critical analysis and review. Biochim Biophys Acta. 2001; 1531:4–46. [PubMed: 11278170]
35. Tanaka M, Koyama M, Dhanasekaran P, Nguyen D, Nickel M, Lund-Katz S, Saito H, Phillips MC. Influence of tertiary structure domain properties on the functionality of apolipoprotein A-I. Biochemistry. 2008; 47:2172–2180. [PubMed: 18205410]

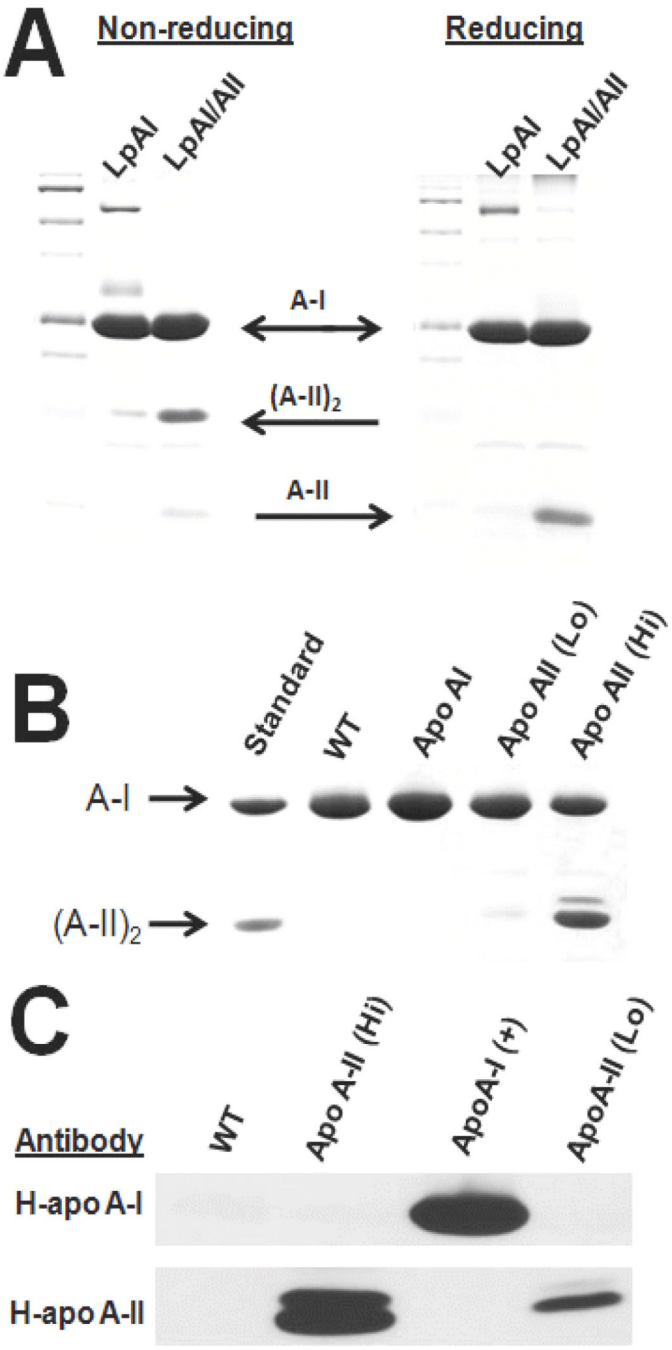

Fig. 1.

SDS-PAGE and Western blots of HDL preparations. A. Coomasie blue staining of LpA-I and LpA-I/A-II as labeled in non-reduced and reduced form following LpA-I and LpAI/A-II isolation by covalent chromatography with TPS. B. Coomasie blue staining of HDL isolated from wild type mice and mice overexpressing human ApoA-I, ApoA-II (Lo), and ApoA-II (Hi) C. Immunoblotting of WT and gene-altered mice as labeled using antibodies to human apo A-I and apo A-II.

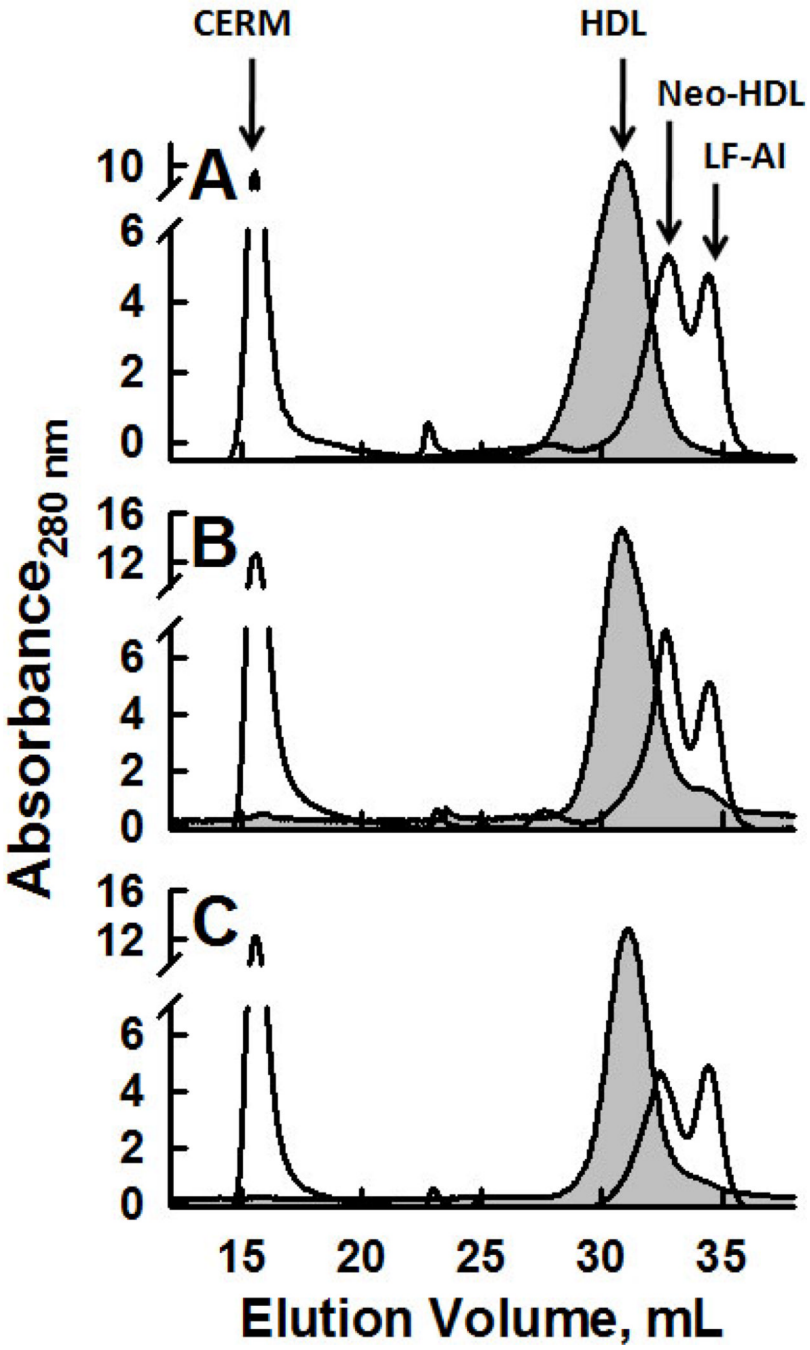

Fig. 2.

SEC of human HDL subfractions pre and post rSOF treatment. A. Total HDL; B. LpA-I; C. LpA-I/A-II. Pre rSOF (grey fill); post rSOF (−). After rSOF treatment, 47%, 42% and 51% of HDL protein was released as LF apo A-I in A, B and C, respectively.

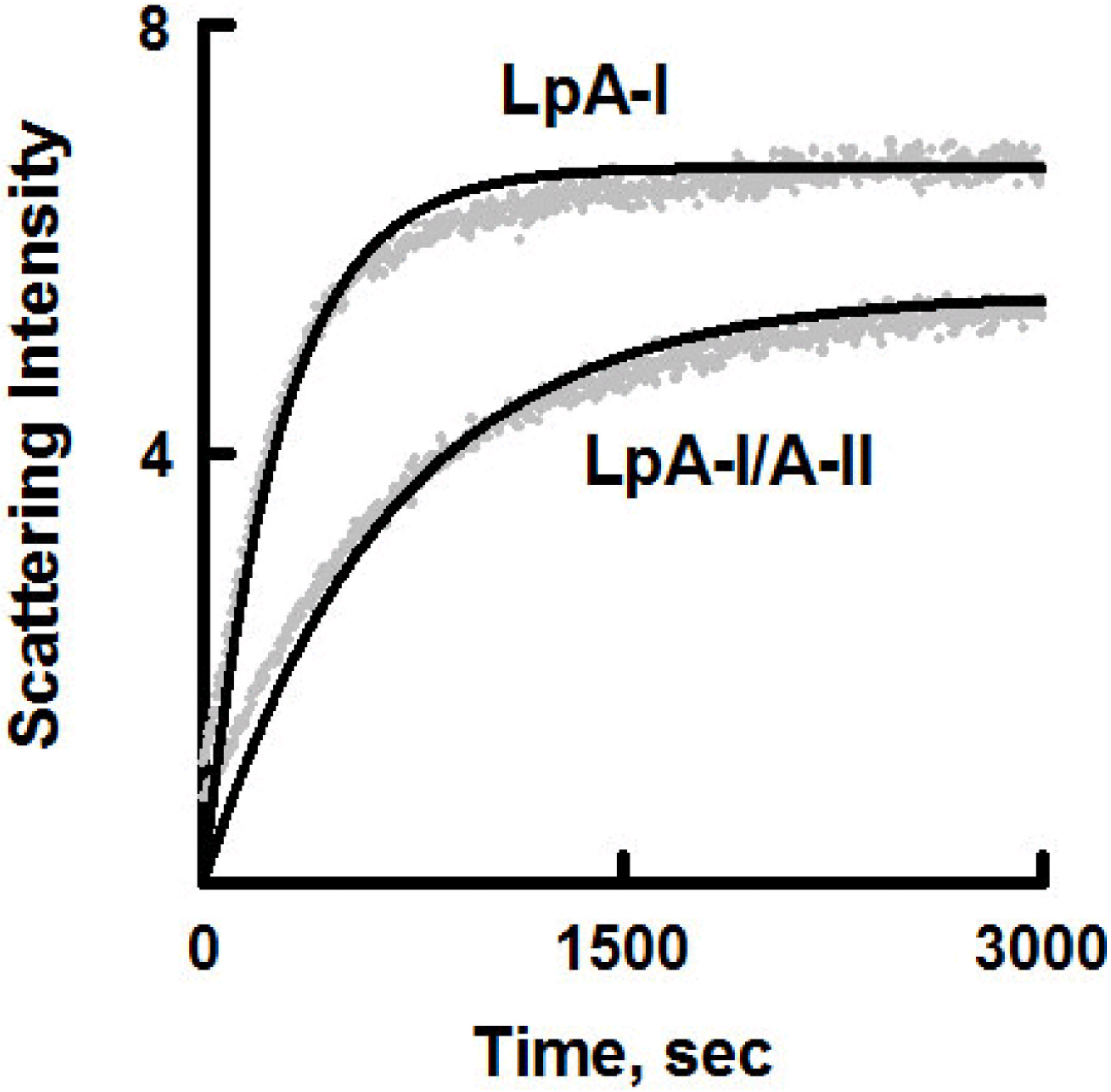

Fig. 3.

Kinetics of Opacification of LpA-I/A-II and LpA-I. The rate constants for opacification of LpA-I (upper curve) and LpA-I/A-II (lower curve) were k = (28.73 ± 0.28) × 10^{-3} sec^{-1} and (11.57 × ± 0.08) × 10^{-3} sec^{-1}, respectively. Data (gray symbols); fitted curve (−).

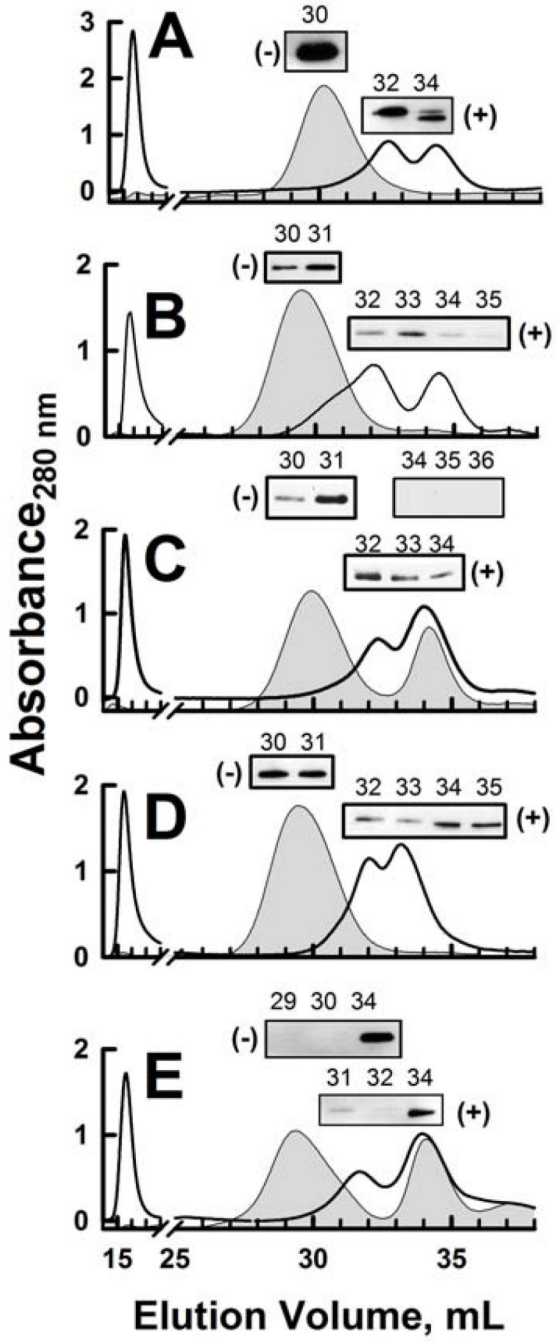

Fig. 4.

Analysis of the effects rSOF on apo-enriched HDL. HDL (0.5 mg/mL) was incubated for 30 minutes at 25 °C with LF apos A-I or A-II and then treated with rSOF (1 μg/mL) for 18 h at 37 °C. The reaction products were separated by SEC and fractions of major peaks were analyzed by immunoblotting. Pre rSOF (grey fill) and upper immunoblot panels; post rSOF (−) and lower immunoblot panels. A. HDL; B. HDL + 0.05 mg/mL apo A-I. C. HDL + 0.23 mg/mL apo A-I; D. HDL + 0.05 mg/mL apo A-II; E. HDL + 0.23 mg/mL apo A-II. The indicated fractions in A, D and E were immunoblotted for apo A-I. Fractions in B and C were immunoblotted for apo A-II. Addition of apoA-I was analyzed for its ability to dissociate ApoA-II from the HDL particle and vice versa.

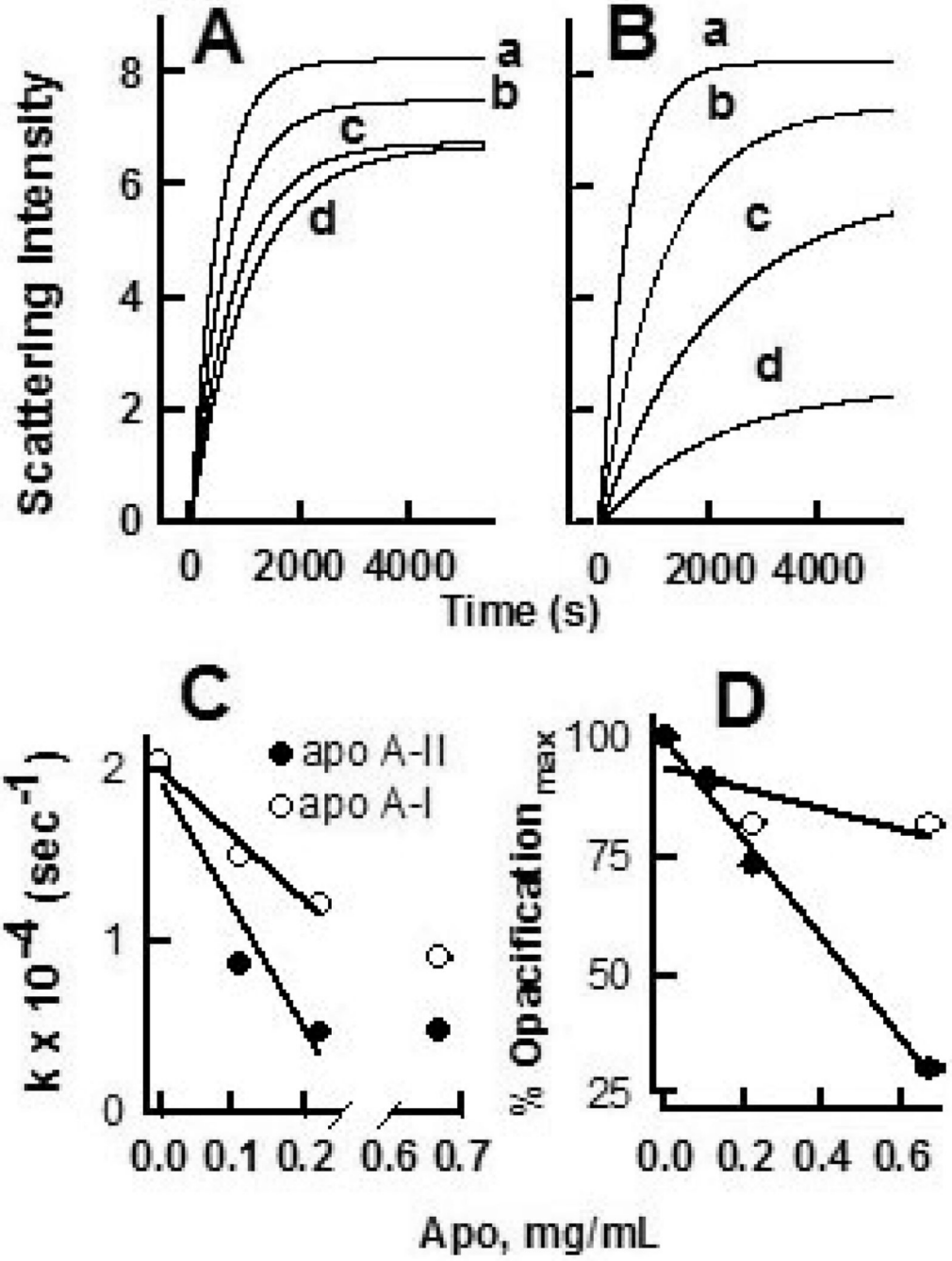

Fig. 5.

Kinetics of opacification of apo-enriched HDL. Opacification kinetics of HDL (0.5 mg/mL) treated with increasing concentrations of (A) apos A-I and (B) A-II. The concentrations of added apos were 0.0, 0.11, 0.23 and 0.67 mg/mL for curves a, b, c and d respectively. Grey points are raw data, black lines are fits to the data using the equation given in the Methods. C. Effect of increasing apo concentration on the rate constant for opacification. For 0.0 to 0.23 mg/mL added apo, the reduction in opacification rate was -7.2×10^{-3} $sec^{-1}mg^{-1}$ for apo A-II and -3.8×10^{-3} $sec^{-1}mg^{-1}$ for apo A-I. D. Maximum opacification of HDL in the presence of added apo A-I or A-II relative to control HDL. For C and D, open circles are addition of apo A-I, closed circles are apo A-II.

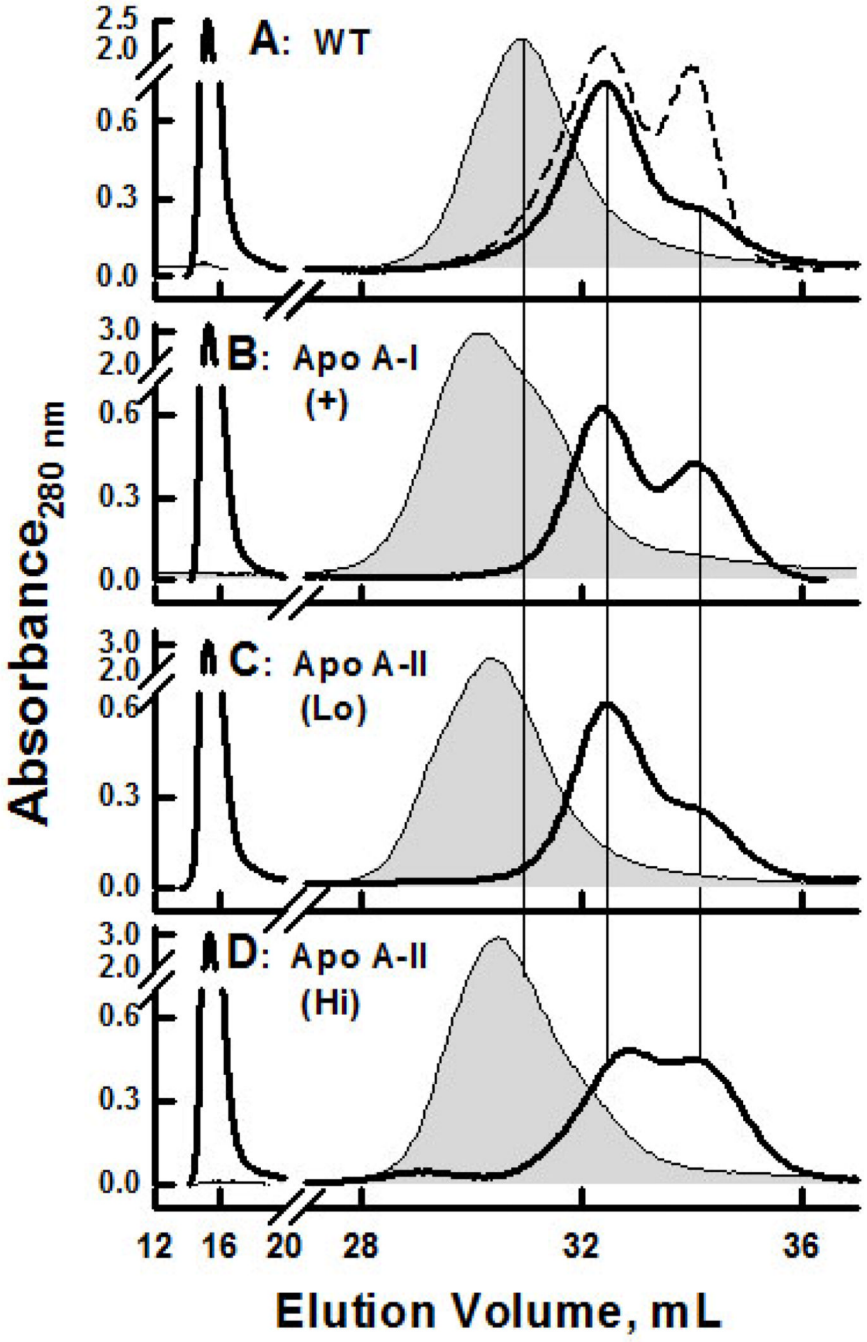

Fig. 6.

SEC analysis of the effects rSOF on HDL from WT and transgenic mice expressing human apos A-I and A-II. rSOF (1 μg/mL) was incubated with HDL (0.25 mg/mL) for 18 h at 37 °C and analyzed by SEC. Pre rSOF (gray-filled curves); post rSOF (−). A. WT; dashed line is SEC trace of rSOF + human HDL from (Figure 2). B. Apo A-I (+); C. Apo A-II (Lo); D. Apo A-II (Hi).

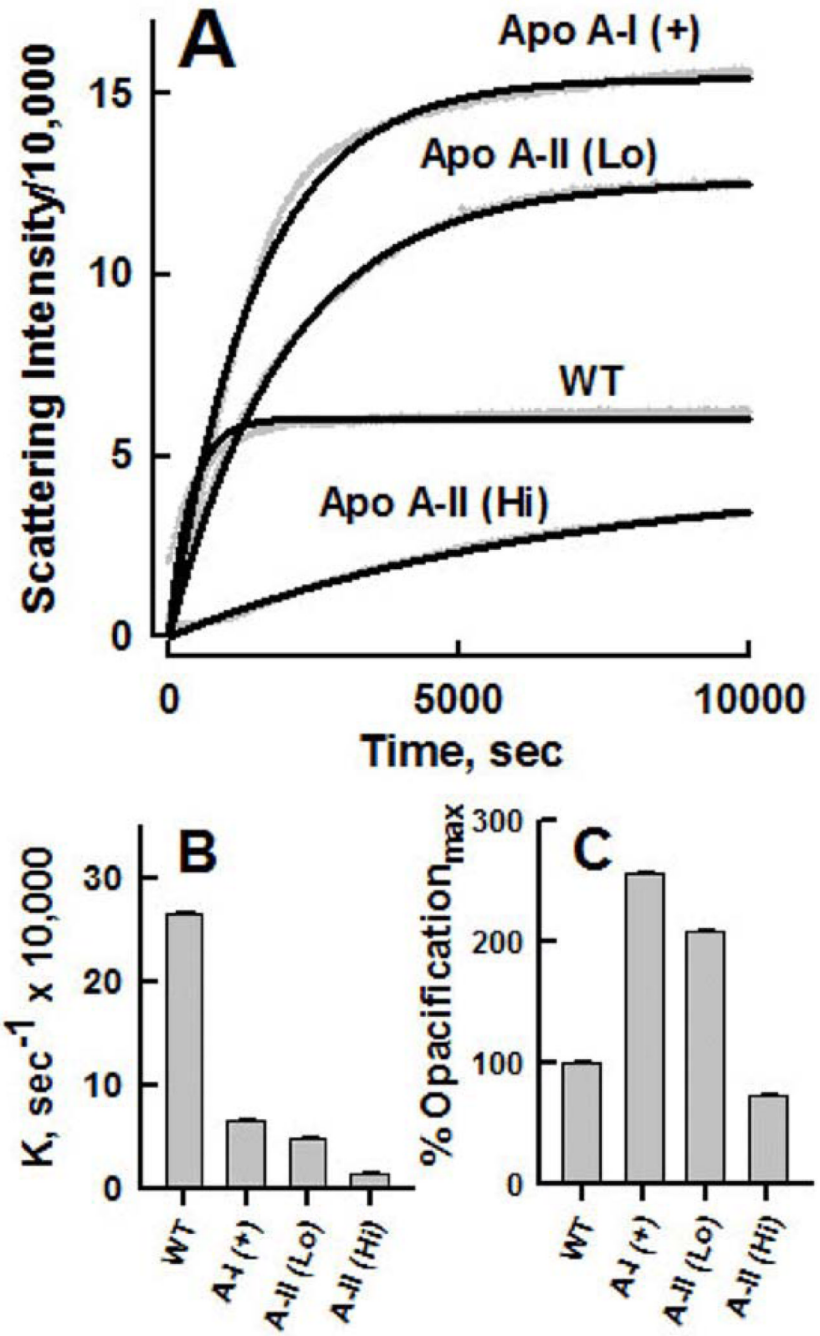

Fig. 7.

Kinetics of opacification of HDL from WT and transgenic mice expressing human apos A-I and A-II. A. Turbidimetric kinetics for mouse HDL (0.5 mg/mL) treated with 1 μg/mL of rSOF as labeled. B. Opacification rate constants for mouse HDL treated with rSOF. C. Maximum opacification relative to WT HDL (= 100%).

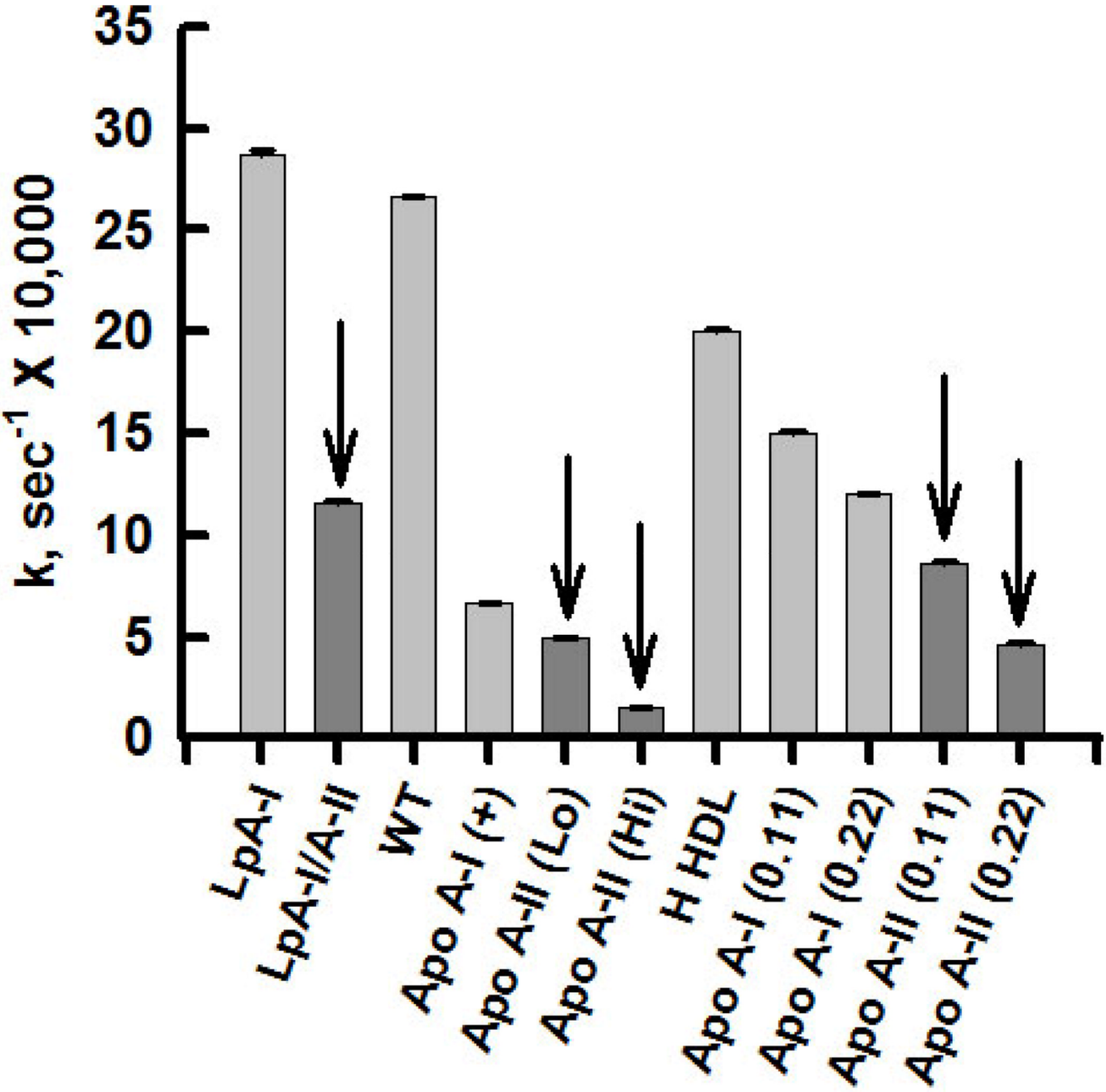

Fig. 8.

Summary of Rate Data. Arrows denote samples rich in human apo A-II. Data compiled from kinetic curves in Figures 3, 5, and 7.